Towards a Non-Intrusive Pulse Oximetry System with Long-Term Mobile Monitoring

by

Mohammad N. Arabi

Electrical and Biomedical Engineering Design Project (4BI6)
Department of Electrical and Computer Engineering
McMaster University
Hamilton, Ontario, Canada

Towards a Non-Intrusive Pulse Oximetry System with Long-Term Mobile Monitoring

by

Mohammad N. Arabi

Electrical and Biomedical Engineering
Faculty Advisor: Prof. M. Jamal Deen

Electrical and Biomedical Engineering Project Report
Submitted in partial fulfillment of the requirements for the degree of
Bachelor of Engineering

McMaster University
Hamilton, Ontario, Canada
March 15, 2010

BACHELORS OF ENGINEERING — McMaster University

(Electrical and Biomedical Engineering) — Hamilton, Ontario

TITLE:	Towards a Non-Intrusive Pulse Oximetry System with Long-Term Mobile Monitoring
AUTHOR:	Mohammad N. Arabi
SUPERVISOR:	Prof. M. Jamal Deen
NUMBER OF PAGES:	47

ABSTRACT

The percentage of arterial oxygen in the blood is a vital physiological sign used by clinicians and doctors to monitor the health of patients under critical conditions in the hospital; the technology used universally to monitor this is known as pulse oximetry. The sensors most commonly used in the hospitals are of reflection type such that the LEDs and the photodetector (PD) are placed on opposite ends of short distance body tissue, e.g. finger.

There has been an increased demand for monitoring patients who have suffered a stroke and are recovering in their homes, and simply the elderly. For such persons, staying in the hospital is unnecessary and undesirable psychologically. As such, a system is to be designed such that patients can monitor their physiological signals, and only contact the doctor when it is imperative to do so. With the comfort of the patient in mind, the system must be unobtrusive in nature such that it does not impede any of their simply daily activities. The sensor used in the system is of reflectance type, i.e. LEDs and PD placed on the same side, and is to be placed on the pectoral region. The pectoral region is chosen for the ease of measuring electrocardiogram (ECG) signals, another vital physiological signal.

Due to lesser blood perfusion in that anatomical region, the question remains as to whether signals could be acquired faithfully there. Results have shown that although signals can be obtained, they vary greatly mainly due to motion artifacts. The system could be improved if complex digital signal processing algorithms are used.

Keywords: Pulse Oximetry, Reflectance Sensor, Motion Artifacts, Wireless, Automatic Gain Control

TABLE OF CONTENTS

1.0 **INTRODUCTION** **6**
1.1 Motivation **6**
1.2 Objectives **6**
2.0 **LITERATURE REVIEW** **8**
3.0 **UNDERLYING THEORY AND METHODOLOGY OF SOLUTION** **10**
3.1 Biological Theory **10**
3.2 Beer-Lambert's Law **11**
3.3 Modeling the Multilayer Tissue **12**
3.4 Pulse Oximetry **14**
3.5 Sensors **17**
3.6 Instrumentation **17**
3.7 Practical Limitations **18**
4.0 **DESIGN PROCEDURES** **20**
4.1 Choice of Sensor **20**
4.2 Sensor Specifications **22**
4.2.1 Physical and Mechanical Specifications **22**
4.2.2 Internal Circuitry **23**
4.2.3 Electronic Specifications of the Sensor obtained Experimentally **23**
4.3 Power Supply **27**
4.4 Operational Amplifier Choice **28**
4.5 Microcontroller Choice **28**
4.6 Oscillator Choice **30**
4.7 LED Control: H-Bridge Configuration **30**
4.7.1 Analog **31**
4.7.2 Digital **32**
4.7.2.1 Microcontroller Integration **32**
4.7.2.2 DC Control **34**
4.8 Transimpedance Amplifier **35**
4.8.1 Photodetector Configuration **35**
4.8.2 Circuit Design **36**
4.9 Sample and Hold Circuit **37**
4.10 Analog Signal Conditioning System **39**
5.0 **RESULTS AND DISCUSSION** **41**
6.0 **CONCLUSION** **43**
REFERENCES **44**
Appendix A: Measurements obtained in calculating the Forward Voltages of the LEDs **45**
Appendix B: Photodetector Output at Different Anatomical Sites and the effects of Ambient Light **47**

LIST OF FIGURES

Figure 1: Optical Absorbance Spectra of Different Gases attached to Hemoglobin in the visible and near-infrared wavelength region.

Figure 2: Model of Skin Tissue: Vasculature imposed. Shades per layer reflect relative absorbance.

Figure 3: Variations in absorption by tissue, and showing the effect of arterial pulsation

Figure 4: Difference between Empirical and Ideal Formulation in relating Ratio R to Oxygen Saturation%

Figure 5: Averaging methodologies that can be implemented. A: Peak-to-peak averaging, B: Step changes along the PPG

Figure 6: Advantages of PureLight technology: 0% contamination below a percent SpO2 of 80

Figure 7: Nonin's 8000R Sensor's Internal Circuitry

Figure 8: Comparison of the Output Current (mA) measured at different sites with the Ambient Light ON

Figure 9: Comparison of the Output Current (mA) measured at different sites with the Ambient Light OFF

Figure 10: LM317T Voltage Regulator

Figure 11: H-Bridge Topology

Figure 12: PWM controlled by Timer 2

Figure 13: H-Bridge Schematic in the Pulse Oximetry System Designed

Figure 14: Time-multiplexing to control the DC output from the transimpedance amplifier

Figure 15: Two modes of operation of a photodiode

Figure 16: Schematic for the Transimpedance Circuit

Figure 17: 3V Precision Sample-and-Hold Circuit

Figure 18: Parallel Implementation of the sample-and-hold circuit

Figure 19: Schematic of the Analog Signal Conditioning System

LIST OF TABLES

Table 1: Six-layer tissue model for nominal blood fraction fo = 0.05.

Table 2: Optical Characteristics of the Tissue Constituents.

Table 3: Leading Sensor Manufacturers

Table 4: Sensor Specifications

Table 5: PIC18F25K20 Specifications

1.0 INTRODUCTION

1.1 Motivation

Pulse oximetry is a universally used method for measuring arterial oxygen saturation reading. This diagnostic tool is heavily favored because it is non-invasive, and provides continuous, safe, and effective monitoring. From a technical perspective, they are almost always maintenance free, require no calibration, and have no side effects on their users [1]. Pulse oximeters do not always have to be used in critical conditions; rather, they can be used as a quick diagnostic tool of a patient at a clinic.

Moreover, Deloitte Consulting has estimated that wireless deployment in the healthcare sector would yield more than 12 billion dollars in the next few years [2]. Few reasons are as follows:

- It directly improves patients' quality of life
- Increases physicians' productivity and efficiency
- Enables freedom of movement for patients
- Can potentially provide a constant link with doctors
- Quick access of information

In this project, the group's concern is providing the patient, in a non-intrusive manner, with quick feedback and easy monitoring of SPO2 and ECG signals to a personal mobile phone since the latter technology is commonly available in every household.

1.2 Objectives

The objective of this project is to design a wireless pulse oximetry monitoring system. The system would be placed at the pectoral region of the patient and would transmit acquired data wirelessly to a mobile phone, PDA, or a laptop computer for fast and easy feedback. With the successful completion of this project, it would potentially be used for continuous home monitoring of persons who have recently suffered cardiac

conditions, or simply the elderly.

The vital physiological signal of concern is the Photoplethysmographic (PPG) signal produced at the output of a photodetector as the result of two LEDs with different wavelengths transmitting light across body tissue. The current output obtained is a function of which LED is transmitting light over an interval of time. An analog circuit is designed to change current outputs to a voltage quantity, to sample-and-hold necessary components, and to filter out unwanted signals. An 8-bit PIC Microcontroller multiplexed with the analog circuitry controls the amount of light emitted from each LED and the timing of the system to separate each current output based on the type of LED transmitting light over an interval of time. Furthermore, the PIC Microcontroller interfaces with a wireless module via the SPI peripheral to send data wirelessly to an electronic device. More details will be provided in the appropriate sections of the report.

Up until the 15th of March, much of the project has been completed, except the last part concerned with the wireless transmission of data. The plan is to complete it within the time left in the winter academic term in 2010.

2.0 LITERATURE REVIEW

The majority of available pulse oximeters require the patient to be lying steadily. Commercial pulse oximeters also use photodetectors that measure **absorption** of light across a short-distance of translucent tissue (e.g. finger tip, earlobe) from two LEDs (red and infrared). The signal is processed and the SPO2 (Saturation of Peripheral Oxygen) level is displayed on a machine usually placed on a counter top close to the patient. Since this method is most accurate, it is used in hospitals for patients in critical conditions. In cases where the patient is not in critical care, but might need constant monitoring from his home, the above- mentioned method is penetrative, intrusive in nature and obstructive to the person's daily chores.

The SPO2 detection method proposed in this design utilizes pulse detection of **reflective** type. As opposed to the absorption method, this can work by placing the sensor of a photodetector and 2 LEDs on the same side of skin, and measuring the reflections of the 2 lights of different wavelengths off a pulsating artery. A direct advantage of this method is that the sensor does not have to be placed across a translucent part of the body; it can work anywhere as long as the tissue it is placed on is well perfused. The pectoral region of the body has been chosen for two reasons:

1 – We needed a complete system that would measure an ECG and an SPO2 signal in a non-intrusive manner. An ECG is best acquired local to the heart.

Research has been done where SPO2 measurements were successfully detected from the pectoral region.

2 – SPO2 measurements recorded at the pectoral region showed a high SNR as opposed to measuring at the wrist. Lower amplitudes are achieved; however, controlling the gain in the data acquisition circuitry can compensate for this [3].

The main problem with placing the pulse oximeter at the pectoral region is the continuous movement of the chest from breathing. Most of the research that has been done to measure SPO2 from that region was on non-moving patients, therefore, this part of the project would be largely experimental. A few preliminary thoughts include:

1 – Displaying to the user the average of a number of signals that have been processed.

2 – Implementing adaptive filtering techniques to reduce motion artifacts. Masimo Corporation has published such a technique [4].

3.0 UNDERLYING THEORY AND METHODOLOGY OF SOLUTION

3.1 Biological Theory

Accurate assessment of blood gases is fundamental to the support of critical-care medicine [1]. It is straightforward to understand that gases like oxygen that are vital to functioning of muscles and organs are carried out in the blood's red blood cells. Moreover, it was discovered in the 1860's that the colored substance in blood, hemoglobin, was also its carrier of oxygen; hemoglobin is a protein that is bound to the red blood cells [5]. At the same time, it was noticed that the absorption of visible light by a hemoglobin solution varied with the different gases attached. The two common forms of the molecule, oxidized hemoglobin (HbO2) and reduced hemoglobin (Hb), have significantly different optical spectra in the wavelength range from 500nm to 1000nm. This means that a light of a certain wavelength (e.g. 660nm) –for example- would be absorbed differently by the red blood cells based on the gases attached to it.

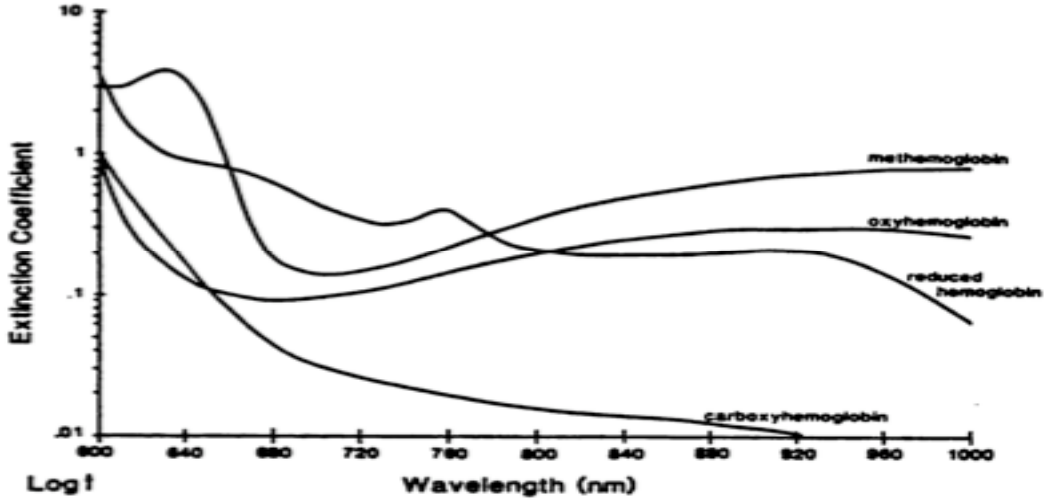

Figure 1: Optical Absorbance Spectra of Different Gases attached to Hemoglobin in the visible and near-infrared wavelength region

The oxygen chemically combined with hemoglobin inside the red blood cells makes up nearly all of the oxygen present in the blood. Consequently the saturation of arterial or peripheral oxygen (SpO2) is defined as the ratio of oxyhemoglobin (HbO2) to

the total concentration of hemoglobin present in the blood. It should be noted that while other gases do exist in the blood, a very large percentage is oxygen, such that the other ones are negligible.

$$\mathbf{SpO2 = HbO2/[Hb + HbO2]}$$

SpO2 is a parameter measured with oximetry and is normally expressed as a percentage. Putting things under perspective, under normal physiological conditions of a healthy individual, arterial blood is 97% saturated.

3.2 Beer-Lambert's Law

The Beer-Lambert law states that the absorbance of light at a specific wavelength by a homogeneous solution can be accurately determined by the following equation:

$$\mathbf{Pt = Po * 10^{-acd}}$$

where 'Pt' is the transmitted light power, 'Po' is the incident light power, 'a' is the specific abosrbptivity of the sample, 'c' is the concentration of the sample, and 'd' is the path length of light. Assuming that the transmission of light through the arterial bed is influenced by the concentrations of HbO2 and Hb only and their absorption coefficients at two measurement wavelengths, then the light intensity will decrease logarithmically with path length according to the Beer-Lambert law [5]. If we consider an artery of length *l* through which light, initially of intensity *Iin* is passed this law tells us that:
at wavelength λ1:

$$I\,1 = Iin(1) * 10^{[ao(1)Co + ar(1)Cr]l}$$

and at wavelength λ2:

$$I\,2 = Iin(2) * 10^{[ao(2)Co + ar(2)Cr]l}$$

where Co is the concentration of oxyhemoglobin (HbO2), Cr is the concentration of reduced (non-oxygenated) hemoglobin, ao(n) is the absorption coefficient of HbO2 at wavelength λn, and ar(n) is the absorption coefficient of Hb at wavelength λn. By

rearranging both equations, we can then derive the formula for calculating the saturation of peripheral oxygen in the blood:

$$SpO2 = Co/[Cr + Co]$$

which is similar to the equation shown above except that it utilizes the Beer-Lambert Law. It is important to keep in mind that this relationship is based on the assumption that the blood artery that light is passing through obeys Beer-Lambert's law, which requires a monochromatic light source and collimated light transmission through the tissue and that the blood does not contain any particles that scatter the light. This of course is an ideality and is definitely not the case with the body tissues and underlying arteries. Therefore, the above equation is an over-simplification. The practical situation is that there is multiple scattering of the light by the red blood cells.

3.3 Modeling the Multilayer Tissue

To deal with such non-ideal issues, we must understand the underlying factors that would affect our signal. Since light of two different wavelengths is to be transmitted to the skin and is expected to hit different peripheral blood supplies (arteries, veins), and other constituents (e.g. fat), we must understand how much is being absorbed or reflected by each respective part. After that is done, we can then have a full grasp of understanding why and how pulse oximetry works the way it does. Since the methodology used in this project is that of reflectance pulse oximetry rather than absorption, the results obtained from a research done by James L. Reuss et al [8] reflect such methodology, i.e. reflectance. The parameters of depth and blood content for six layers in the tissue as obtained by the Reuss et al. are found in Table 1.

Table 1. Six-layer tissue model for nominal blood fraction $f_0 = 0.05$

Layer (i)	Name	d_i (cm)	f_i
1	Epidermis	0.02	0
2	Dermis (non-perfused)	0.02	0
3	Papillary plexus	0.02	0.0556
4	Dermis (perfused)	0.08	0.0417
5	Cutaneous plexus	0.06	0.2037
6	Hypodermis	0.80	0.0417

This model is better shown in Figure 2 with the grey scale reflecting blood content and consequent relative absorption per layer. Furthermore, the vascular vessels are superimposed on the image. This should help visualize the anatomy and physiology better.

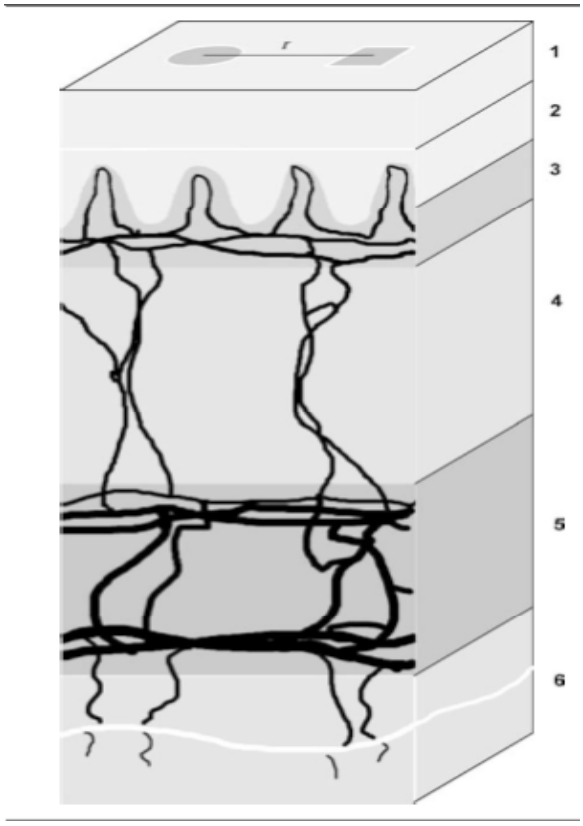

Figure 2: Model of Skin Tissue: Vasculature imposed. Shades per layer reflect relative absorbance.

Moreover, the utmost concern is in regards to the optical characteristics of the tissue constituents. In relation to this project, Reuss et. Al obtained the following results with a reflective pulse oximeter sensor. The results are displayed in Table 2. The two LEDs used were a red one (660 nm) and another near-infrared one (890nm).

Table 2: Optical Characteristics of the Tissue Constituents

Variable	Meaning	660 nm	890 nm
μ_a (HHb)	Absorption, deoxy. Hb	17.139	4.595
μ_a (O_2Hb)	Absorption, oxygenated Hb	1.692	6.309
μ_a (tissue)	Absorption, non-blood tissue	0.285	0.245
μ_a (melanin)	Absorption, melanin	269.440	99.558
μ_s	Scattering, blood and tissue	71.5	44.5
g	Anisotropy	0.8	
n	Refractive indices (internal)	1.3	

It is clear from the results shown above that we have absorption from reduced and oxidized hemoglobin; however, the largest absorption comes from melanin. Melanin is a dark pigment responsible for the tanning of the skin. This of course is subject-dependant; however, it will be shown in the next section that such a result does not have a big impact as its effect will be removed.

3.4 Pulse Oximetry

To overcome the problems mentioned in section 3.2, a revolutionary method was introduced by Aoyagi et al. [6] and Yoshiya et al. [7]. As explained in the previous section, pulse oximetry assumes that the attenuation of light by the body segment can be split into three independent components: arterial blood, venous blood and tissues. Our signal of interest is the time-variant Photoplethysmographic (PPG) signal caused by changes in arterial blood volume directly associated with heart contraction. Note that at the time following heart contraction, oxygen-rich blood is sent to the tissues and organs in the body though arteries. Pulse oximetry makes three assumptions [1] as follows:

1 – The time-variant PPG signal is attributed solely to the arterial blood component,
2 – The PPG is sensitive to changes in arterial oxygen saturation,
3 – There is no pulse from the surrounding vascular bed – venous blood does not pulsate

As such, we can calculate the SpO2 by analyzing the changes in absorbance at two different wavelengths. Referring to Figure 1 and Table 2, it is clear that using LEDs of different wavelengths (e.g. red and IR at 680nm and 940nm respectively), would give different absorbance levels in different molecules.

Analyzing the results obtained in the previous section, and Table 2 specifically, it is also clear that tissue absorption is a large factor and this is expected to vary from one person to another. Also, transmitted light intensities depend on the detector sensitivity and intensities of the individual LEDs. As such, we can expect the output to have both DC (non-pulsatile) and AC (pulsatile) components. As expected, the AC component is the result of the time-changing PPG signal due to arterial absorption. The DC component is composed of light absorbed by tissue (e.g. melanin) and venous blood. Refer to Figure 3.

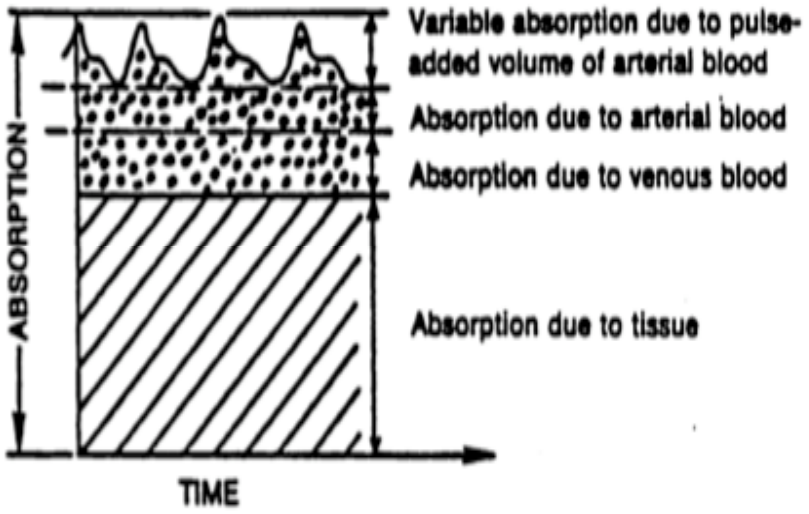

Figure 3: Variations in absorption by tissue, and showing the effect of arterial pulsation

Since the DC components vary widely between subjects, a normalization process is required for each light of different wavelength. This ratio would be largely independent of incident light and other unneeded factors.

For two different wavelengths, R would be represented as such:

$$R = \frac{\log_{10}\left(\left(I_{dc+ac}\right)/\left(I_{dc}\right)\right)_{\lambda 1}}{\log_{10}\left(\left(I_{dc+ac}\right)/\left(I_{dc}\right)\right)_{\lambda 2}}$$

The relationship between R and SpO2% is based on empirical data; look-up tables are usually used to calculate the SpO2% for a subject. Note that this relationship gives different results than the ones obtained using the Beer-Lambert ideal equation. This is shown in Figure 4.

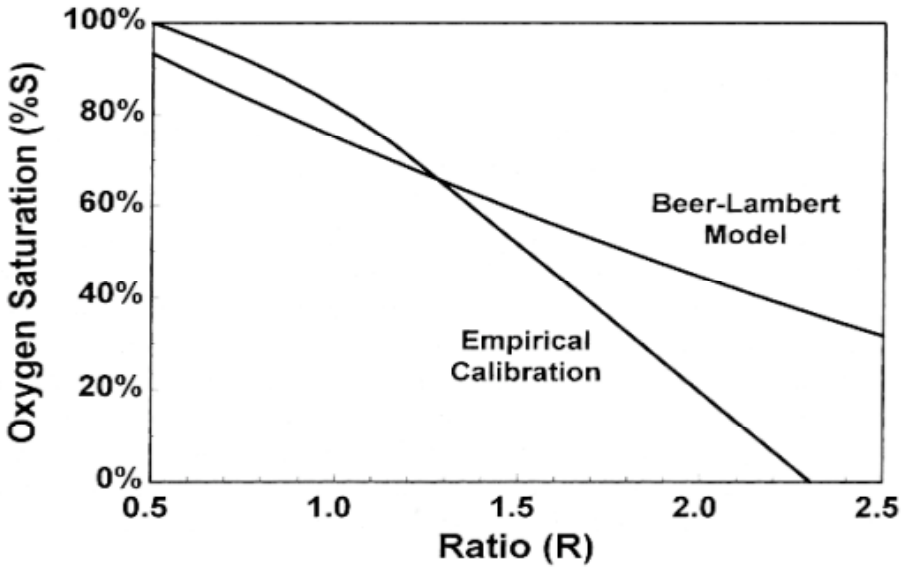

Figure 4: Difference between Empirical and Ideal Formulation in relating Ratio R to Oxygen Saturation%

3.5 Sensors

Two types of sensors are commercially available:

1 – Transmittance type: a pair of red and infrared LEDs and a single photodetector mounted on the opposite side. The arterial bed is therefore in between. The sensor is mounted in a spring-loaded clip or an adhesive wrap.

2 – Reflectance type: the LEDs and the photodetector are mounted on the same side facing the skin. The most common place for mounting the sensor is the forehead.

3.6 Instrumentation

To have a complete working pulse oximetry system, a microcontroller is needed to switch the power of both LEDs such that they are not both on at the same time. Moreover and simultaneously, the microcontroller demultiplexes with respect to time he red and infrared the outputs from the photodetector corresponding to their respective LEDs. The signals are then filtered to obtain the time-varying pulsatile PPG signal that is sent to the microcontroller for processing and looking the ratio R from the look-up table.

An important note is that the response of the pulse oximeter depends on the number of data points averaged by the oximeter before the final saturation percentage is displayed; there are two basic approaches to averaging [1]:

1 – Time average of the peak-to-peak amplitudes of each pulse – this is slow.

2 – Average many step changes along the steep slopes of the PPG – this is much faster.

This is shown better in figure 5.

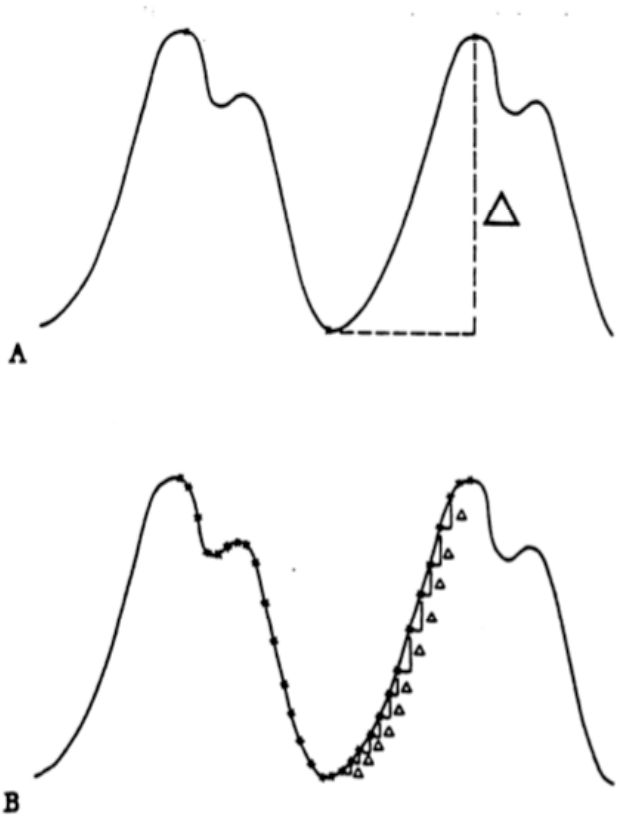

Figure 5: Averaging methodologies that can be implemented. A: Peak-to-peak averaging, B: Step changes along the PPG

3.7 Practical Limitations

Pulse oximetry is a technology used to constantly monitor patients in hospitals, or more recently for individuals in their homes. Over a long period of time, many irregularities could happen with the patient that would limit the functionality of the pulse oximetry instrumentation system. Such limitations [1] may include:

1 – Low vascular perfusion: In situations of vasoconstriction, hypotension, or other similar conditions where the heart does not beat strong enough to pump blood sufficiently to the tissues, a PPG signal would be too small to be detected reliably or accurately. As expected, noise in this case would have a much greater effect on the signal too. While a

ratio R may not be calculated accurately for use in the look-up table to display to the user, the pulse oximetry can display a ‘Low Perfusion’ message to the user.

2 – Motion Artefacts: Any motion of the sensor relative to the skin can cause a significant change in the PPG signal. The effects of motion artefacts is a major problem and can be dealt with by digital signal processing and/or averaging the PPG values over an interval of time before displaying the final result to the user. In cases where motion is extreme, a message could be displayed to the user indicating that.

3 – Interference of background light: The reading of the pulse oximeter may be affected by surrounding light sources since the photodetector may be respond to such ambient light. Off-the-shelf sensors are usually wrapped with a dark material and have cases designed to minimize such interference.

4.0 DESIGN PROCEDURES

4.1 Choice of Sensor

This was the first thing that I had to buy to get the design of the system going. Many factors contributed to the choice of sensor made, and this will be discussed in detail in this section. For this project, I was looking for a reflectance type sensor. Commercially, those are most commonly sold as forehead reflectance sensors. The leading companies involved in the design and distribution of the sensors include:

1 – Nonin Medical , 2 – Covidien: Nellcor, 3 – Masimo, 4 – NuMed Holdings, 5 – Radianse, and 6 – OB Scientific, Inc.

Table 3: Leading Sensor Manufacturers

Manufacturer	**Reflectance Sensor**
Nonin Medical	8000R Sensor
Covidien: Nellcor	OXIMAX MAX-FAST, RS-10
Masimo	LNCS Forhead Sensor
Numed Holdings Ltd.	-
Radianse	-
OB Scientific, Inc	-

It should be noted that in most papers that I have read, the researchers have custom-made their sensors on to a Printed Circuit Board (PCB). This involved many details as to the shape of the PCB, the number and orientation of LEDs with respect to the photodetector and vice versa. Moreover, if I were to design the sensor, I would have to make a mechanical structure for the PCB that would secure position and avoid ambient light. Although this would be the cheapest way to go about this, it would require most time and is highly prone to error. As such, I have decided to buy an off-the-shelf sensor.

With this decision now established, I had five criteria to decide which sensor to buy. They were:

1 – Price, 2 – Availability, 3 – Compatibility, 4 – Connector Type, 5 – Availability of Data. By 'Compatibility', I mean if the sensor would be compatible with any personal designed circuitry. The 'Availability of Data' field refers to if I have extra information about the sensor (e.g. circuitry).

The results were as follows from the three companies.

Table 4: Sensor Specifications

Manufacture	**Sensor**	**Price**	**Availability**	**Compatibility**	**Connector Type**	**Availability of Data**
Nonin Medical	8000R	165 CAD	Yes	Yes	D-SUB-9	Yes – Circuit Diagram and Information on website
Covidien: Nellcor	RS-10	200 CAD	Yes	Yes – Includes an RCal	D-SUB-9	Yes – Circuit Diagram
Covidien: Nellcor	MAX-FAST	-	-	No – New Technology	-	-
Masimo	LNCS - 989803148311	594 CAD	-	-	-	-

From the table above, it is clear that my two choices were limited between Nonin's 8000R sensor and Nellcor's RS-10. The 8000R sensor is cheaper and I have more information about it; I chose the Nonin's 8000R sensor.

4.2 Sensor Specifications

4.2.1 Physical and Mechanical Specifications

The following information is provided from Nonin Medical's website [9]. The sensor has two LEDs and 1 photodetector (PD). The red light has a wavelength of 660nm, and the infrared one has a wavelength of 920 nm. Both LEDs are made by Nonin's PureLight® sensors. What is special about PureLight® technology is that the red LED does not produce a secondary spectrum emission. Consequently, this does not cause 'contamination' impacting oxygenated haemoglobin measurement, and there would be no variation in readings below an SpO2 percentage of 80%. Nonin's PureLight sensors eliminate variations in readings from patient to patient. This is not the case with other LEDs as is shown in the figure below.

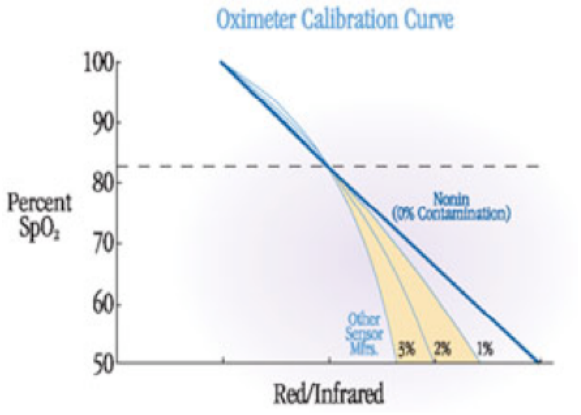

Figure 6: Advantages of PureLight technology: 0% contamination below a percent SpO2 of 80

The sensor is considered a reusable one and ideal for stress testing and spot-checks. The disadvantage of this sensor, however, is that when it is worn for a long period of time, sweat would accumulate and it will have to be removed, cleaned, then fit on the patient again. The sensor can be wiped with Isopropyl alcohol, which is the commonly found 'rubbing alcohol', found in households. From the patient's perspective, the sensor is comfortable and comes with 10 adhesive collars to ensure proper placement.

4.2.2 Internal Circuitry

The internal circuitry as provided by Nonin's Engineers is as follows:

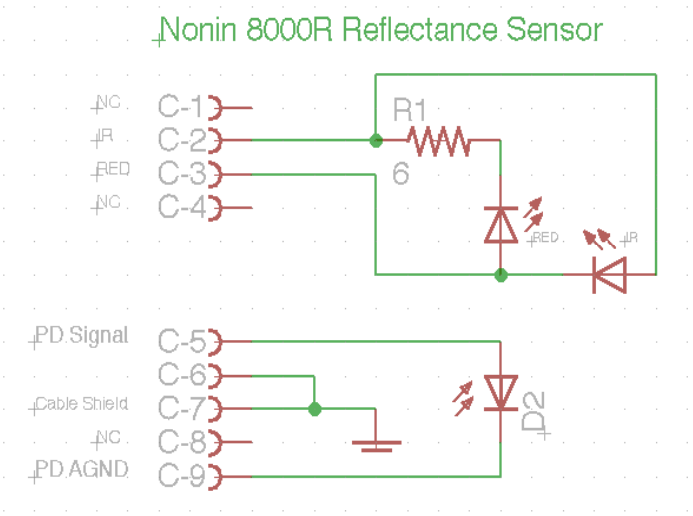

Figure 7: Nonin's 8000R Sensor's Internal Circuitry

It is relatively easy and straightforward to see how this sensor works. When the voltages at pins 2 and 3 of the connector are equal, neither LED turns on. When the voltage at pin-3 is higher than that of pin-2, the red LED turns on. When the voltage at pin-2 is higher than pin-3, then infrared LED turns on.

4.2.3 Electronic Specifications of the Sensor obtained Experimentally

The sensor did not come with a data sheet for me to look up the exact specifications of the sensor. Since the sensor would integrate with the analog circuitry and the microcontroller, I had to find the forward voltage to turn on each LED experimentally. Moreover, I had to perform tests to find out the magnitude of the current output from the PD at different anatomical sites (e.g. index finger, forehead, and the chest) and the effect of ambient light on the PD.

For the first type of experiment, I needed a 1kohm resistor, an ammeter, and a variable voltage supply.

Forward Voltage of Red LED:

The 1kohm resistor and the ammeter were placed in series before pin 3. The variable voltage supply was placed across pins 2 and 3, with the positive supply placed on the latter pin. The result is that current would flow from the positive voltage supply through the 1kohm resistor, then the ammeter, to the sensor, and back to pin 2. The voltage supply is powered at 0V and increased steadily until current changes on the ammeter and the red LED turns on. Measurements were taken at different points, each time recording the voltage and the current. These measurements can be found in the appendix.

The result was that the forward voltage of the red LED was roughly equal to 1.4V and was calculated easily using the equation:

$$Vd = Vs - iR;$$

Where Vs is the supply voltage, Vd the forward voltage, 'i' is the current measured at the ammeter, and R is the equivalent resistor placed in series.

Forward Voltage of IR LED:

The same procedure was used for the infrared LED, except that this time we could not see the LED turn on. Also the resistor in series used was equal to 470 ohms. Similarly, the voltage and the current were recorded at different points as the voltage was increased. These measurements can be found in the appendix.

The result was that the forward voltage of the infrared LED was roughly equal to 1.1V

Measuring current output at Different Anatomical Sites and the effects of Ambient Light

For this experiment, a transimpedance circuit was quickly built to change output current from the PD to voltage. This could be easily implemented by placing a resistor in parallel with the PD at the positive input an op-amp. Voltage at the input of the op-amp is then equal to V = i*R1. R1 was equal to 10kohm. A further voltage gain of 100 is added in the negative feedback of the op-amp by using two resistors of values 100kohm and 1kohm. The total gain in the circuit was therefore 1M V/V.

Due to lack of time, this experiment was only performed with the **red LED!** Extending from the previous experiment, the transimpedance circuit was connected to the PD, and the voltage was measured at the output of the op-amp using the oscilloscope set to 'DC Coupling.' The following results were obtained. Tabulated measured data can be found in the appendix.

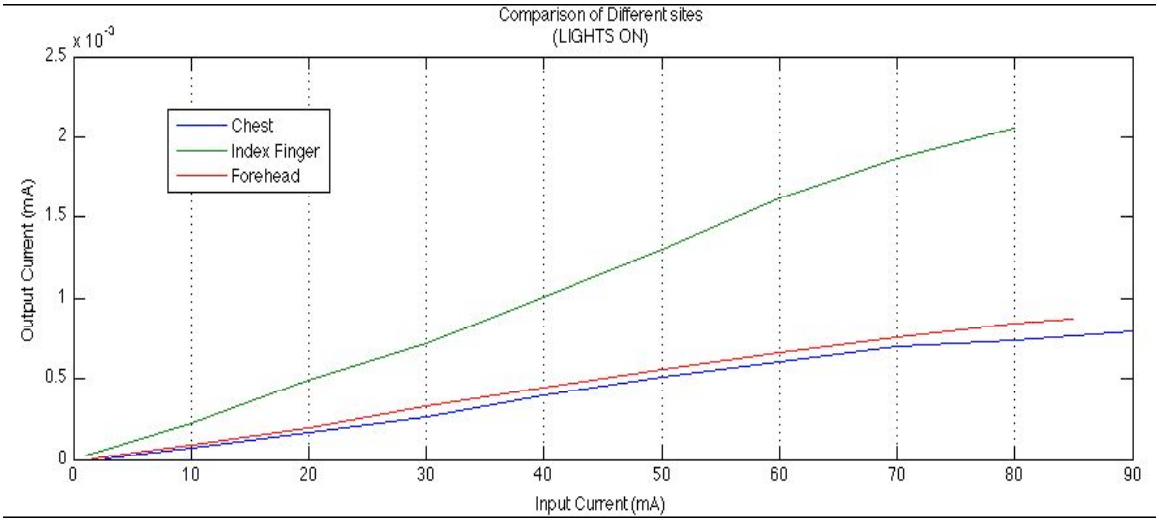

Figure 8: Comparison of the Output Current (mA) measured at different sites with the Ambient Light ON

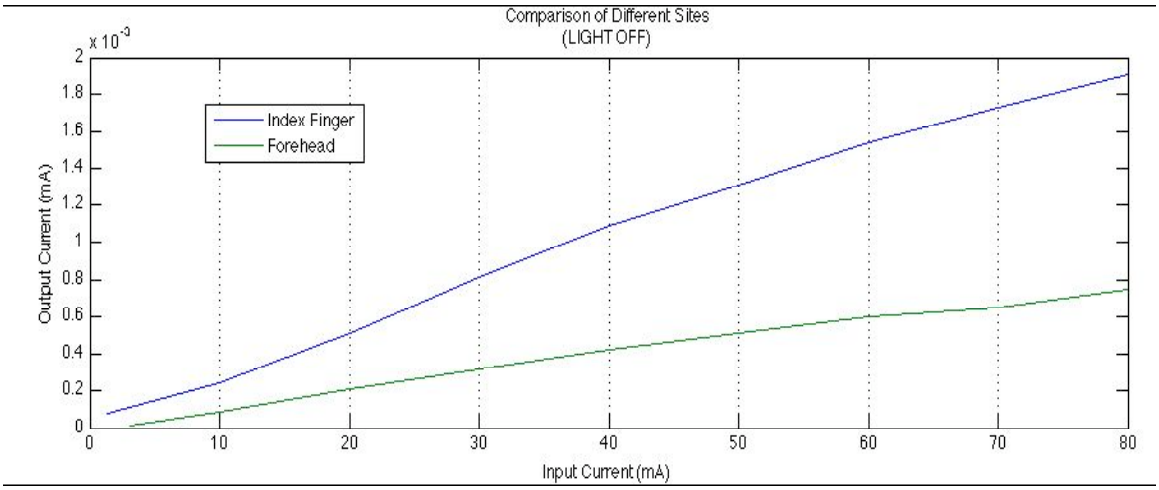

Figure 9: Comparison of the Output Current (mA) measured at different sites with the Ambient Light OFF

Due to lack of time, I was not able to continue the experiment for the chest. This does **not** mean that results are unobtainable from the chest when the light is turned off. It is clear from the experiments that ambient light does have a small effect even when the sensor is placed securely against the anatomical part. It should also be noted that this experiment was done to the same one subject.

Using the results of the experiment, I know what to expect to see at the output of the PD when a certain magnitude of current input is supplied to the LEDs. It is also important to note that since the oscilloscope was configured to 'DC Coupling', I was able to see both DC and AC components; however, the AC component was extremely small compared to it, and therefore the average of the signal was equal to the DC component.

Referring to section 3.3 of the report, we can safely say that the output current at the index finger was higher because it is most rich in vascular arteries. For the same reason, the output measured at the forehead was higher than that measured at the chest.

4.3 Power Supply

The objective is that the system is used unobtrusively, and naturally, a battery-operated system is the way to go. Moreover, to maximize the life of the battery and the system, the circuit should be powered from a constant low voltage source. Most Integrated Circuits are currently manufactured to be powered from as low as 3V. The system was designed such that it is powered from a 9V standard battery. A regulated voltage supply is needed for the circuit to operate properly. Therefore, a voltage regular is needed, and I chose National Semiconductor's LM317 3-terminal adjustable regulator. Another regulator that I could have chosen was the famous National 7805 voltage regulator. The reason why I chose the LM317 was because it is adjustable and can supply voltages as low as 1.2V, and supply currents up to 1.5A, which is more than needed. The 7805 regulator would only supply a constant 5V and a current up to 1A. Since the LM317 was available and priced at 0.7CAD, I did not hesitate in choosing it. It was used as follows:

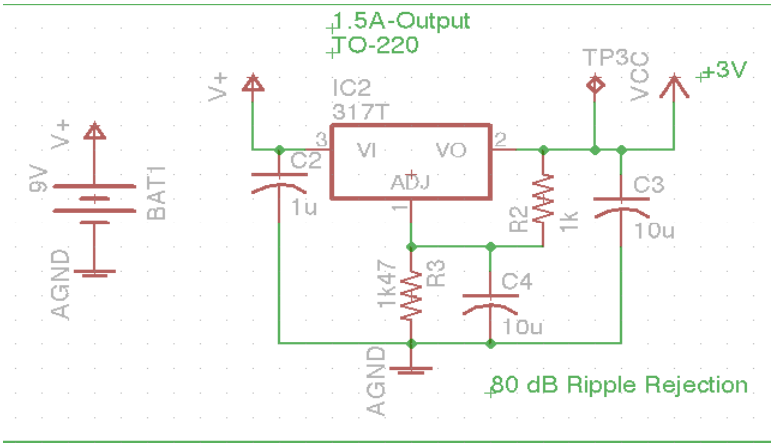

Figure 11: LM317T Voltage Regulator

Tantalum capacitors were placed at the inputs and outputs to improve ripple rejection. The 10uF output capacitors would provide up to 80 dB of ripple rejection.

4.4 Operational Amplifier Choice

The operational amplifier (op-amp) used in this system was Analog Devices' general-purpose quad OP491. This op-amp was chosen because it can work in single supply operation from as low as 2.7V, which guarantees that it would work at 3V. It has a low supply current of 300uA/amp, and the output voltage can swing to within millivolts of the supplies. Such properties make it ideal for battery-powered instrumentation. Moreover, its ability to swing rail-to-rail at both the input and the output allows to build multistage filters and to maintain high signal-to-noise ratios [11]. The op-amp was quite expensive and priced at 7.91CAD.

4.5 Microcontroller Choice

Many different microcontrollers are found in the market that would do perfectly for this application. Famous companies that are leaders in manufacturing microcontrollers include Microchip, Atmel, and Texas Instruments. A microcontroller is a complex semiconductor device with many integrated peripherals, and is often programmed from the computer using software (Development Environment) provided by the company. The program code can be either written in C-code or basic level instruction language. To transfer the code on to the chip, a programmer is needed to compile and build the code into HEX data and bits that the microcontroller would 'understand' and use. The number and types of peripherals embedded, and the price and availability of physical tools needed to use the microcontroller efficiently are important factors that must be considered when choosing the microcontroller.

Texas Instruments manufactures the ultra-low power MCU: MCP430™. It utilizes a 16-bit RISC architecture and consumes less current than its counterparts from competitive companies (e.g. PIC24F). It also has many peripherals and integrated circuits embedded within it, which would lessen external analog circuitry. The ultimate problem with such a microcontroller is that the external tools needed to program it are not free, and not many sources are available to help in using the chip to its full potential. Moreover, it may have more than is needed, and this would be wasteful.

Atmel Corporation has a wide variety of microcontrollers to choose from and would be highly competitive with Microchip. Many resources are also available for free that would help in optimizing the use of the microcontroller. The main reason why I limited my research furthermore to Microchip PIC microcontrollers was because the latter company manufactures XLP (extreme Low Power) ones that would be ideal for use in battery-operated systems.

When limiting the solutions to PIC microcontrollers with XLP technology, I would have choices between PIC12s, PIC16s, PIC18s, and PIC24s. All of PIC12, PIC16 and PIC18 uC series utilize 8-bit RISC architecture as opposed to the 16-bit PIC24; however, the PIC18 series are C-code optimized (can be programmed using C advanced programming language) and usually have more program memory. I was able to obtain a PIC18F25K20 from a friend for free along with the PICkit 2 Development Programmer. The main properties of this uC that would be of help in this project can be found in the table below:

Table 5: PIC18F25K20 Specifications

Parameter Name	**Value**
Operating Voltage	1.8-3.6V
Case	PDIP
XLP	Yes
Pin Count	28
Digital Communication Peripherals	1-A/E/USART, 1-MSSP(SPI/I2C)
Capture/Compare/PWM Peripherals	1 CCP, 1 ECCP
ADC	10 ch, 10-bit
Program Memory Type	Flash
Internal Oscillator Clock	16MHz
In-Circuit Serial Programming	Single Supply (3V) via 2 pins

4.6 Oscillator Choice

The oscillator for the system is directly related to the supply voltage of the uC system. Since the system is powered at 3.0V, the uC clock could range from as high as 20MHz to 64 MHz; it could of course run at lower clock speeds. Furthermore, there can be different sources for the oscillator: internal or external. The external clock modes using a crystal can provide accurate speeds up to 64KHz. This of course would consume more power. The internal oscillator clock provides a speed of 16MHz and can be reduced to 8MHz by changing the correct bit in the control register. A Phase-locked Loop circuit can also be used to multiply the internal oscillator speed by 4. This means that using the internal oscillator, I could have the following timer speeds: 8,16,32 (8*4), and 64 (16*4) MHz. Such an advantage may eliminate the need for an external oscillator. It should be noted that the main disadvantage is instability: the frequency of the timer may drift as the supply voltage and temperature change.

Since my concern is to have a working prototype, and high speeds are not crucial, the 16MHz internal oscillator seems sufficient enough. This reduces the power supply and the cost of buying a crystal.

4.7 LED Control: H-Bridge Configuration

Since the LEDs will be switching and will not turn on at the same time, an H-bridge configuration seems to be the best topology for implementing such a process. It also integrates easily with the uC via the ECCP (Enhanced Capture, Compare, PWM) peripheral. The general topology for an H-bridge is shown in the figure below.

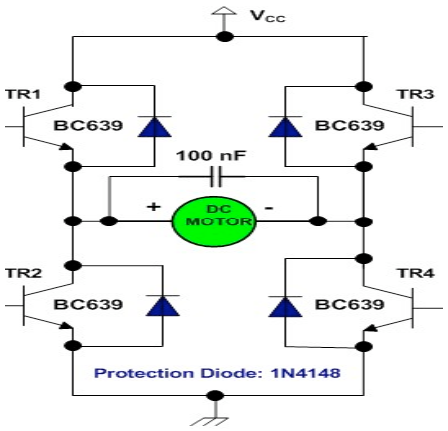

Figure 12: H-Bridge Topology

4.7.1 Analog

It is known that the transistor has 3 regions of operation: On, Off, Saturation. However, to use the transistor effectively as a switch, it must only go through two regions of operations: Off and Saturation. The 'off' state can be easily obtained by not supplying any current to the base of the transistor. The saturation state is obtained by supplying enough current to the base of the transistor such that the collector current is nearly constant.

Also, the H-bridge could be built using both NPN and PNP transistors. In this system, I have decided to only use NPN transistors for the following two advantages:

1 – NPN transistors have a faster turn-on time

2 – Similar transistor characteristics in the circuit

The NPN transistors used in this application were Fairchild Semiconductor's PN2369A switching transistors. This device is designed for high speed saturated switching at the collector of currents 10mA to 100mA. The maximum power dissipation for the transistors at room temperature is 350 mW. I decided to run a current of 65mA through each LED; referring to previous results in section 4.2.3, this would give a DC output of roughly 660mV. This could be easily amplified and processed later. Since the H-bridge is to be powered at 3V, the power dissipation of the H-bridge when either LED is turned on is P = 3*65m = 195 mW, which is less than the maximum power dissipation.

The next step is to choose the correct resistors. The gain of each transistor is 85 V/V, and so the base current needed to give a constant collector current of 65mA is equal to 65mA/85 = 0.75mA which is much lower than the current that each pin at the uC can source/sink (185mA). The digital high voltage at the output pins of the uC is 2.3V and the base-emitter drop voltage is 0.92V; therefore, the resistor should be equal to R = (2.3 – 0.92)/0.75m = 1840 ohm. 1/4W size resistors should be sufficient for this purpose.

4.7.2 Digital

4.7.2.1Microcontroller Integration

The advantage of integrating the H-bridge with the microcontroller is that we can utilize the use of the ECCP peripheral, and more specifically the full-bridge configuration of PWM. With Pulse-Width Modulation, we can increase or decrease the intensity of the LED by changing the duty cycle of the signal input.

The heart of the ECCP peripheral is the Timer 2 peripheral, which is used as a counter for generating PWM pulses. The pre-scale circuit, that can be selected using the T2CKPS1 and T2CKPS0 bits in the T2CON register, supplies the TMR2 counter register clock. The TMR2 register value is compared to the PR2 register which determines the top value of TMR2 counter register. When the TMR2 value is equal to the PR2 value, the TMR2 counter register is reset to 0. At the same time, the value of TMR2 counter register is compared to the CCPR1L register value, and when the TMR2 value is equal to it, the PWM peripheral circuit resets the CCP1 output (logical “0“). Similarly, when the TMR2 counter register is equal to the PR2 register, it sets the CCP1 output high (logical “1“). It is clear to see that by changing the PR2 value we could change the PWM period; this means changing the PWM frequency too [12]. This is shown in the figure below.

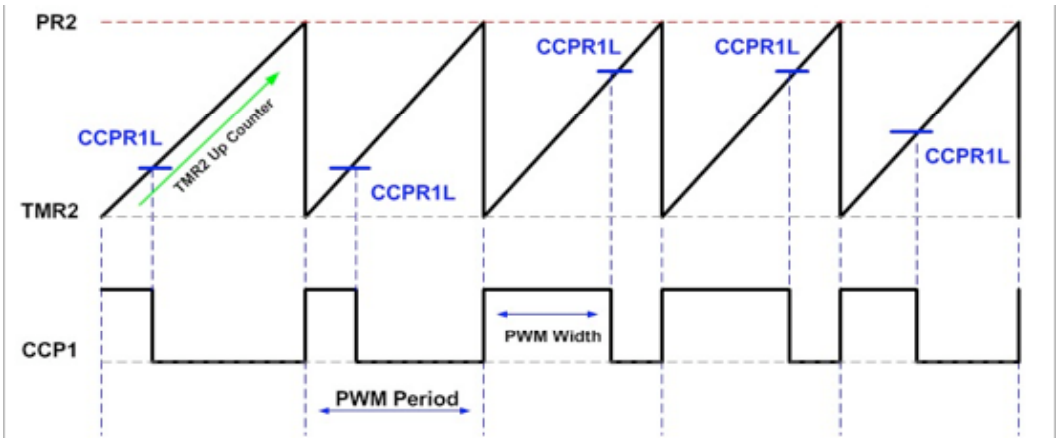

Figure 13: PWM controlled by Timer 2

In this system, the pulse width is equal to 50us at a repitition rate of 500Hz.
The PWM period can be calculated using this following formula:

PWM period = (PR2 + 1) x 4 x Tosc x (TMR2 prescale value) second;
where Tosc is the system clock period in seconds

The PWM width can be calculated using this following formula:
PWM width = (CCPR1L:CCP1CON<5:4>) x Tosc x (TMR2 pre-scale value) second

The CCP1CON, PWM1CON and PSTRCON registers control the PWM output behavior. Note that all the TRIS (three states input/output) registers for each of the PWM output ports: P1A, P1B, P1C and P1D should be cleared or set to output mode.

Since the H-bridge is used in full-mode, it can be set in forward direction and reverse direction. This can be set using the P1M<1:0> registers in the CCP1CON register set. Furthermore, for this design, all pins are set to active high by changing register CCP1M<3:0> in the CCP1CON register set.

The schematic of the H-bridge used in the design is as follows:

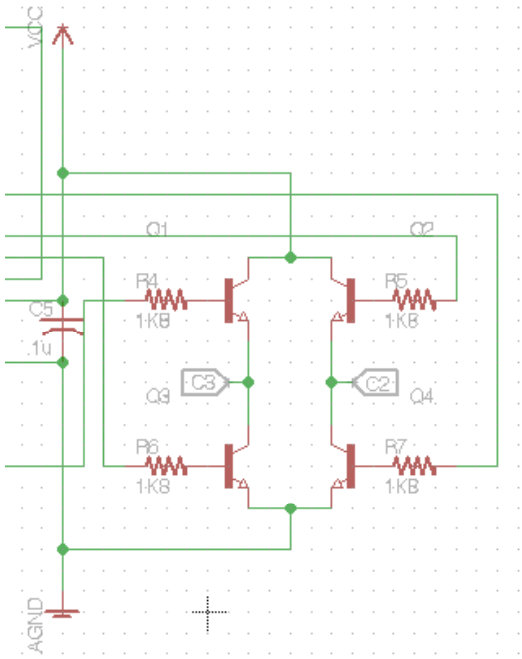

Figure 14: H-Bridge Schematic in the Pulse Oximetry System Designed

4.7.2.2DC Control

PWM will also help in giving the same DC offset from both LEDs. This way the AC constituent of the PPG only matters. Referring back to section 3.4, it is clear from the formula provided that the Ratio R has the DC components of the different wavelengths in the denominator of both fractions. If we can set the DC component for each LED respectively to give a constant DC supply of 2V, then that value will cancel out of the ratio, and ratio R will then be equal to the ratio of the AC components at different wavelengths. There are three main advantages to such a design:

1 – This will be subject-independent

2 – The DC component can be cut-off using a high-pass filter and only the AC output will be processed

3 – The analog signal conditioning system will have fixed parameters because the AC output will be known.

This is implemented in the system such that the output of the transimpedance amplifier will be directly sent to an ADC channel in the microcontroller. Because the timers control which LED turns on when, we can find out which part of the output belongs to which LED. Also recall that although the output will have both AC and DC components, the average of the signal will just be DC. That DC value is compared to 2V, and the intensity of that respective LED is changed accordingly to give a stable output of 2V next 'time'. The idea for such an implementation was obtained from a TI application note on pulse oximetry [13].

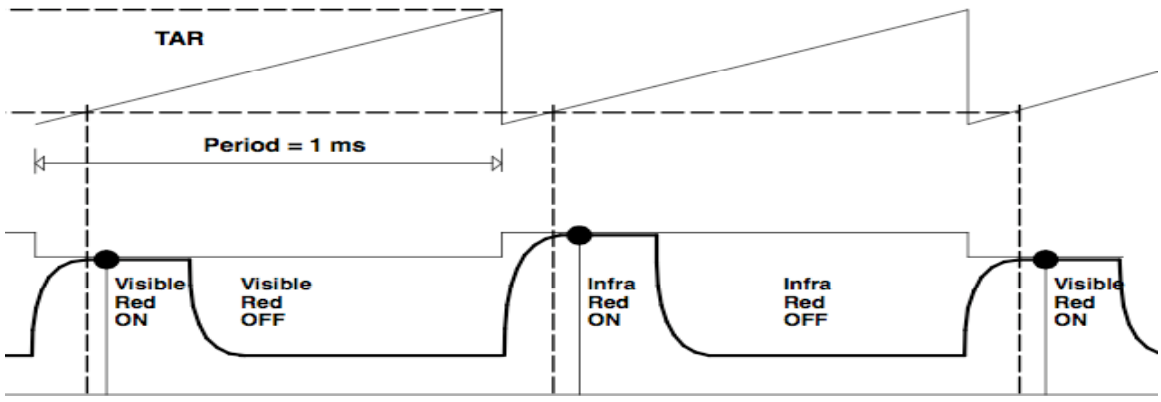

Figure 15: Time-multiplexing to control the DC output from the transimpedance amplifier

4.8 Transimpedance Amplifier

4.8.1 Photodetector Configuration

The photodetector can be placed in the circuit using either of the two modes: Photovoltaic or Photoconductive. In the Photovoltaic mode, the photodiode is biased with zero volts, which optimizes the sensor's accuracy.

In the Photoconductive mode, the diode is reverse biased in order to optimize the responses to step functions [10]. The two configurations are as follows:

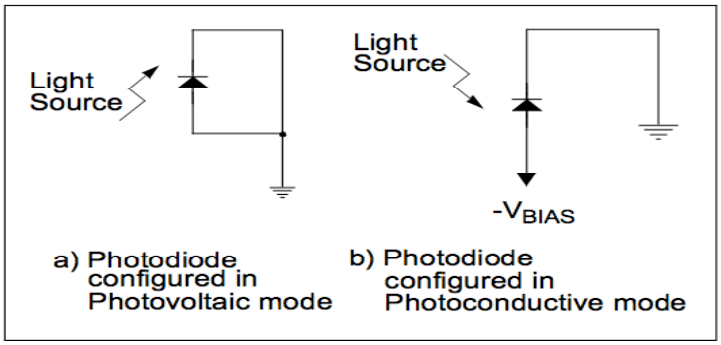

Figure 15: Two modes of operation of a photodiode

The photodetector was configured in Photovoltaic mode for the following reasons: PPG are not fast changing signals and their highest frequency component is empirically estimated at 5Hz. Precision is preferred in this case over response time and speed. Moreover, in Photovoltaic mode, there is less leakage current, and noise and DC errors are minimized. Such factors are extremely important especially that we are interested in the time-varying pulsatile AC signal that has a very small magnitude.

4.8.2 Circuit Design

The PD has an inherent output capacitance that can affect the circuit response. Since we are primarily working at low frequencies, the capacitor is merely an open circuit, and does not play an important role in the circuit response. Nonetheless a 3pF capacitor is placed in the negative feedback loop of the capacitor to improve stability if it was affected significantly originally. This capacitor can be changed at any time if the system is found to be unstable.

As mentioned in section 4.7.1, a current of 60-65 mA is to be passed through the LEDs. Referring to Appendix B, it can be seen that the output current of the PD at the chest is equal to 610 nA. Therefore to have a major DC output of 2V, we need to pass the current through a resistor of value equal to V/I = 2/610n = 3.3 MOhm. Furthermore, we must consider the op-amp's input bias current and offset voltage. When the OP491 is powered at 3V, the bias current is equal to 30nA while the offset voltage is equal to 80uV. Their effect on the current output is equal to:

30nA + 80u/3.3M = 30nA. The resultant error in the output current is therefore: 30/610 = 4.9%, which is an acceptable and tolerated number.

The schematic of the transimpedance circuit is as follows:

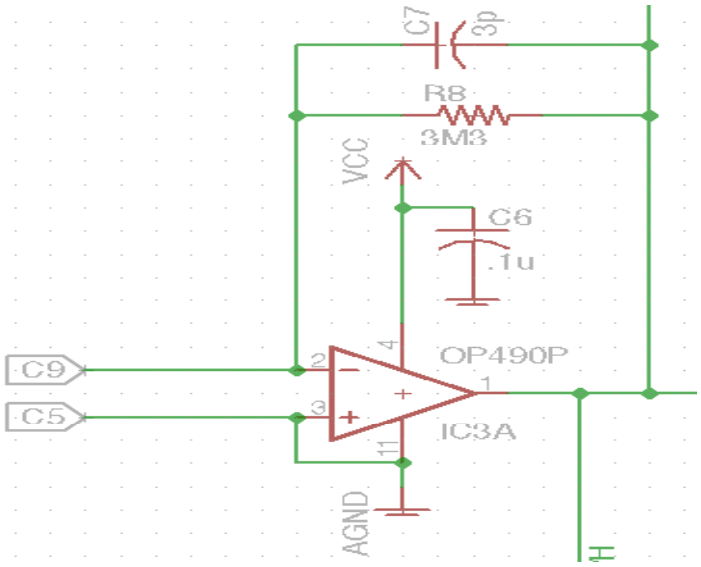

Figure 16: Schematic for the Transimpedance Circuit

4.9 Sample and Hold Circuit

As it has been shown in Figure 15, the output of the transimpedance amplifier will include both infrared and red components. The output is then taken to two different parallel sample-and-hold circuits that each would sample according to which light is turned on. Effectively, the same output is taken to identical sample-and-hold circuits, but each circuit samples at a different time, and therefore, the output of the sample-and-hold circuit is different for the parallels.

The design of the sample-and-hold circuit was taken from an op-amp's data sheet under the Applications section [14]. The schematic is shown in the figure below.

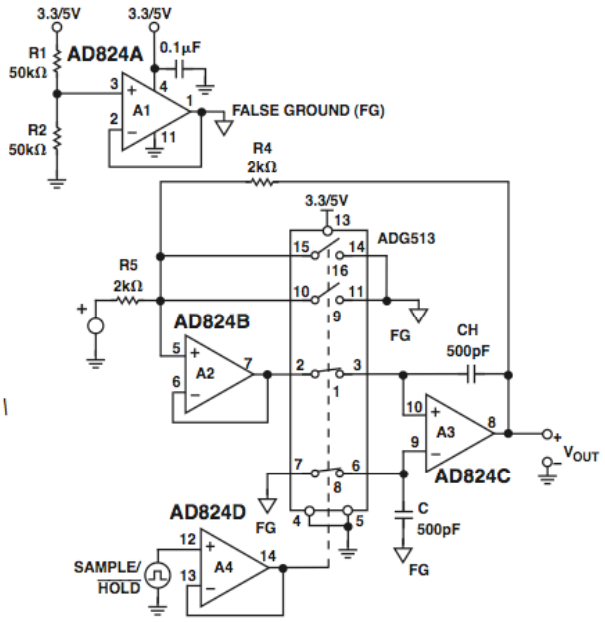

Figure 17: 3V Precision Sample-and-Hold Circuit

CH and C2 were chosen to be 500pF Teflon capacitors since such caps exhibit low leakage and a low dielectric absorption. In the design of my circuit, instead of the ADG513 shown above, I used MAXIM's 4066 Low-Voltage, Quad, SPST (Single Pole, Single Throw) Analog Switches. The ADG513 were not available at the manufacturer of choice, namely DigiKey. However in the 4066, switches are normally open, and to make internal switches 2 and 3 opposite to switches 1 and 4 – as shown above – the HCF4007 Inverter, manufactured by STMicroelectronics, was used. To better visualize its implementation in the system, refer to the figure below.

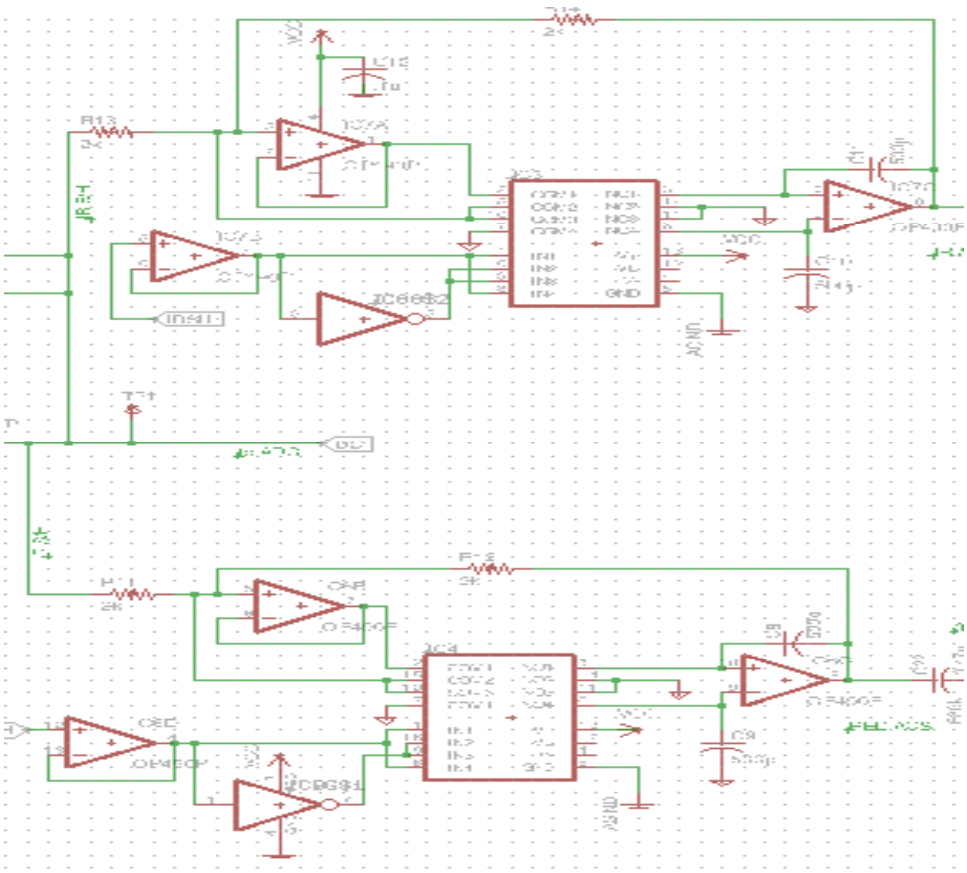

Figure 18: Parallel Implementation of the sample-and-hold circuit: The output of each SH circuit is different and corresponds to each LED

4.10 Analog Signal Conditioning System

The analog signal conditioning system was straightforward. The DC component of the signal had to be removed, and for that a simple first order high-pass filter with a cut-off frequency of 0.5Hz was used. Since the system is powered form 0-3V, the AC component of the signal had to be raised such that the virtual ground was equal to 1.5V. As such, all originally analog ground connections were replaced with the false ground of 1.5V. A fourth-order Butterworth Filter with a cut-off frequency of 5Hz and a gain of 100 was implemented. A big advantage to this system is that it gets rid of the 50-60Hz-noise signal that can easily couple on to the circuit. The Butterworth configuration was chosen because it has a flat pass band response as opposed to the Tchebycheff filter.

It should be noted that the analog signal conditioning system was implemented twice corresponding to the different PD outputs. The schematic of the analog conditioning system can be seen below.

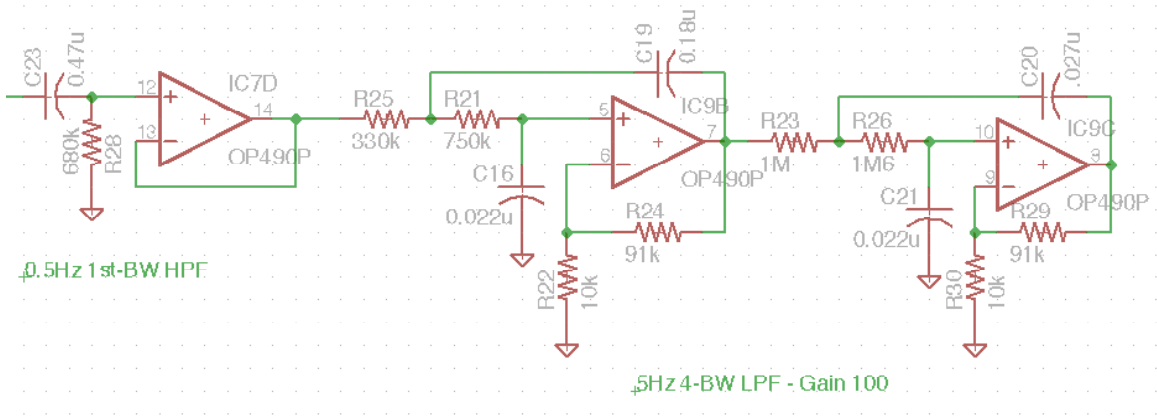

Figure 19: Schematic of the Analog Signal Conditioning System

The output of the analog signal conditioning system interfaces with the uC via the ADC peripherals.

5.0 RESULTS AND DISCUSSION

The system has not been completed to perfection yet, and there is still some work left to do with the microcontroller. Some of the work left to do includes perfect timing and multiplexing of the circuit; an example of that would be stopping ADC acquisition when the output of the transimpedance amplifier goes back to zero. These details could be implemented, and will hopefully be taken care of at the end of the academic term.

Another aspect that has not been worked on is the wireless system. A wireless module is readily available at Microchip and would interface with the uC via the Serial Peripheral Interface (SPI) Peripheral. MiWi protocol would be implemented at radio frequency since it uses a point-to-point network and a low bit-rate. The solution is cheap and sufficient for our purposes.

The AC signal of the PPG was captured successfully; however, it does not seem to be very stable. That is the results change instantaneously and significantly when the sensor is moved slightly. Moreover, different results were obtained when the sensor was placed at different places on the sternum, although theoretically they should give the same result since the vascular system is the same in that region. The results are as follows:

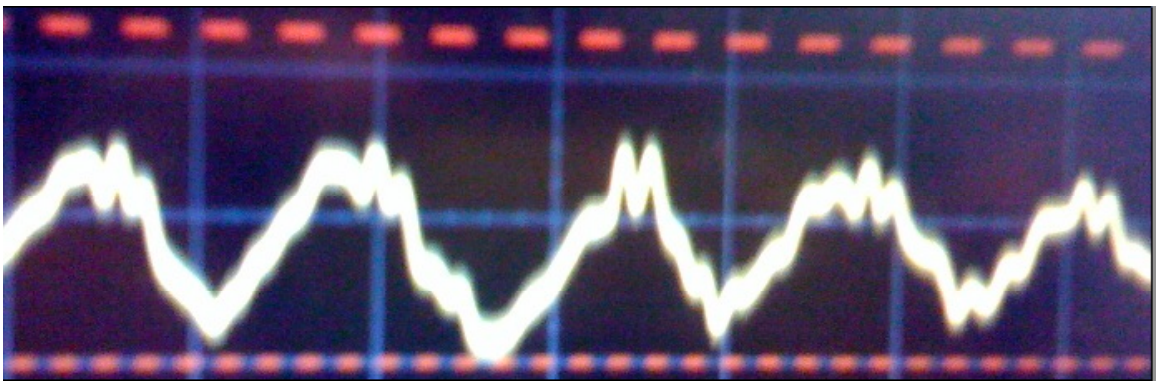

Figure 20: AC component of the PPG signal measured at the lower sternum

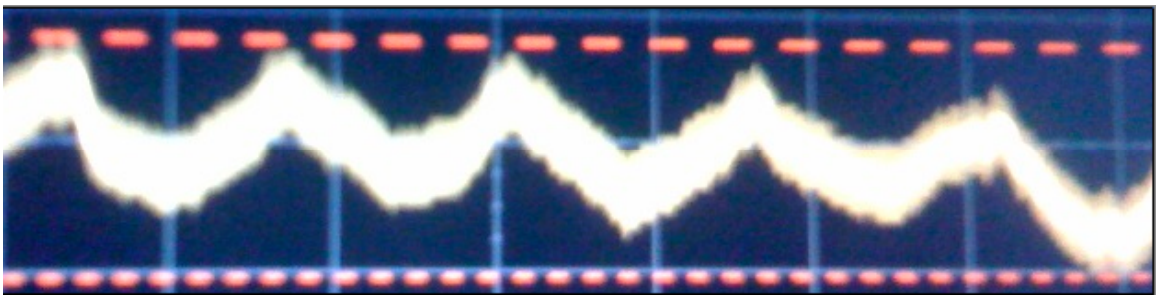

Figure 21: AC component of the PPG signal measured at the upper sternum

From the results shown above, it is obvious that the results shown in Figure 21 are much noisier and more importantly, the AC component is less significant. More controlled experiments may have to be performed and recorded. Moreover, every time the subject inhaled and exhaled, the PPG signal would change.

Moreover, the instrumentation system could be improved if digital signal processing is implemented as opposed to the analog counterpart. The filters would be much improved, and more importantly, the parallel analog circuits for processing the red and the infrared outputs could be simplified to a much simpler one. Practically, Microchip provides dsPIC chips that support digital signal processing, and those could be implemented to optimize the system.

6.0 CONCLUSION

The system could definitely be optimized in the future for more intricate circuitry and more complex Digital Signal Processing algorithms. A solution must be found to remove or greatly reduce the effects of motion artefacts caused by the chest moving due to breathing for the system to be used as a long-term solution.

Other ways the system could be optimized is by modifying the sensor topology such that there would be more than one photodetector circulating two LEDs in an attempt to capture all reflected light since the underlying tissue may not be homogenous.

REFERENCES

[1] Mendelson Y. Pulse oximetry: theory and applications for noninvasive monitoring. Clin Chem. 1992; 38(9): 1601-1607.

[2] Moron MJ, Casilari E, Luque R, Gazquez JA. A wireless monitoring system for pulse-oximetry sensors. IEEE CS. 2005; 79-84.

[3] Maattala M, Konttila A, Alasaarela E, Chong WY. Optimum place for measuring pulse oximeter signal in wireless sensor-belt or wrist-band. ICCIT. 2007; 1856-1861.

[4] Graybeal JM, Petterson MT. Adaptive filtering and alternate calculations revolutionizes pulse oximetry sensitivity and specificity during motion and low perfusion. IEEE EMBS. 2004; 5363-5366.

[5] Medical Electronics, Dr. Neil Townsend, Michaelmas Term 2001

[6] Aoyagi T, Kishi M, Yamaguchi K, Watanabe S. Improvement of earpiece oximeter. In: Abstracts of the Japanese SocietMedical Electronics and Biological Engineering, 1974:90-1.

[7] Yoshiya I, Shimada Y, Tanaka K. Spectrophotometric monitoring of arterial oxygen saturation in the fingertip. Med Biol Eng Comput 1980; 18:27-32.

[8] James L. Reuss, Daniel Siker. The Pulse in Reflectance Pulse Oximetry: Modelling and Experimental Studies. JCMC 2004; 18:289-299.

[9] http://www.nonin.com/

[10] Baker B. Using a Digital Potentiometer to Optimize a Precision Single-Supply Photo Detection Circuit. Microchip Technology Inc; AN692

[11] OP191/291/491 Data Sheet: Micropower Single-Supply Rail-to-Rail Input/Output Op Amps

[12] http://www.ermicro.com/blog/?p=706

[13] Chan V, Underwood S. A Single-Chip Pulse Oximeter Design Using the MSP430. Texas Instruments 2005; SLAA274

[14] AD824 Data Sheet: Single-Supply, Rail-to-Rail, Lower Power, FET-Input Op Amp

Appendix A: Measurements obtained in calculating the Forward Voltages of the LEDs

Following are the voltage and current measurements recorded for calculating the forward voltage of the **red LED**

Voltage Supply (V)	**Ammeter Current (mA)**
1.43	0.012
1.46	0.02
1.5	0.033
1.68	0.128
1.73	0.163
1.8	0.216
2.05	0.412
2.2	0.5
2.7	1.0
3.2	1.423
3.5	1.7
3.87	2.19

Following are the voltage and current measurements recorded for calculating the forward voltage of the **infrared LED**

Voltage Supply (V)	**Ammeter Current (mA)**
0.813	0.001
0.929	0.01
970	0.02
1.043	0.058
1.124	0.135
1.25	0.297
1.533	0.716
1.7	1.008
2.12	2.0
2.63	3.0
3.09	4.0
5.965	10.0

Appendix B: Photodetector Output at Different Anatomical Sites and the effects of Ambient Light

The following data shows the input current used to power the LED, and the voltage measured at the output of the transimpedance amplifier with a gain of 1M V/V. Therefore, to calculate the output current of the PD, the outputput voltage must be divided by the gain.

Anatomical Part: Index Finger
Ambient Light: ON

Input Current (mA)	Output Votlage (V)
1.0	0.022
10.0	0.220
20.0	0.490
30.0	0.720
40.0	1.01
50.0	1.30
60.0	1.62
70.0	1.864
80.0	2.053

Anatomical Part: Forehead
Ambient Light: ON

Input Current (mA)	Output Votlage (V)
1.6	0.0006
10.0	0.092
20.0	0.200
30.0	0.330
40.0	0.448
50.0	0.560
60.0	0.659
70.0	0.756
80.0	0.844
85.0	0.870

Anatomical Part: Chest
Ambient Light: ON

Input Current (mA)	Output Votlage (V)
2.7	0.0036
10.0	0.068
20.0	0.168
30.0	0.262
40.0	0.400
50.0	0.508
60.0	0.610
70.0	0.702
80.0	0.740
90.0	0.793

Anatomical Part: Index Finger
Ambient Light: OFF

Input Current (mA)	Output Votlage (V)
1.3	0.0783
10.0	0.2376
20.0	0.513
30.0	0.811
40.0	1.0919
50.0	1.308
60.0	1.5378
70.0	1.729
80.0	1.909

Anatomical Part: Forehead
Ambient Light: OFF

Input Current (mA)	Output Votlage (V)
3.1	0.0139
10.0	0.0869
20.0	0.2067
30.0	0.312
40.0	0.4204
50.0	0.511
60.0	0.596
70.0	0.651
80.0	0.751